

# Merging Solid-Phase Peptide Synthesis and Automated Glycan Assembly to Prepare Lipid-Peptide-Glycan Chimeras

Manuel G. Ricardo<sup>[a]</sup> and Peter H. Seeberger<sup>\*[a, b]</sup>

Biomaterials with improved biological features can be obtained by conjugating glycans to nanostructured peptides. Creating peptide-glycan chimeras requires superb chemoselectivity. We expedite access to such chimeras by merging peptide and glycan solid-phase syntheses employing a bifunctional monosaccharide. The concept was explored in the context of the on-resin generation of a model  $\alpha(1\rightarrow6)$ tetramannoside linked to peptides, lipids, steroids, and adamantane. Chimeras containing a  $\beta(1\rightarrow6)$ tetraglucoside and self-assembling peptides such as

FF, FFKLVFF, and the amphiphile palmitoyl-VVVAACKK were prepared in a fully automated manner. The robust synthetic protocol requires a single purification step to obtain overall yields of about 20%. The  $\beta(1\rightarrow6)$ tetraglucoside FFKLVFF chimera produces micelles rather than nanofibers formed by the peptide alone as judged by microscopy and circular dichroism. The peptide amphiphile-glycan chimera forms a disperse fiber network, creating opportunities for new glycan-based nanomaterials.

## Introduction

Carbohydrates and proteins are classes of macromolecules that mediate biological processes through distinct mechanisms. Insights into their chemical structures and functions have enabled unique applications, as well as highlighted inherent pharmacological limitations.<sup>[1,2]</sup> By combining both biopolymers into a single synthetic construct, their biological parameters can be altered. In glycoconjugate vaccines, poorly immunogenic bacterial polysaccharides are linked to proteins that provide T-cell help (e.g. non-toxic diphtheria toxin CRM197).<sup>[3,4]</sup> Selective targeting of cancer cells with peptides combined with the antibody recruiting capacity of some glycans improves anti-tumor performance.<sup>[5–8]</sup>

The multivalent presentation of glycans on supramolecular architectures potentiates binding affinity and molecular recognition.<sup>[9,10]</sup> Different biomolecular chimeras combine glycan fragments with self-assembling peptides,<sup>[11–13]</sup> among other systems.<sup>[9,14–16]</sup> Lipid tails appended to beta-sheet-forming peptides result in peptide amphiphiles that form a dense nanofiber network simulating extracellular tissues.<sup>[17–19]</sup> Such

lipopeptides have been decorated with glycans<sup>[12]</sup> and nucleic acids,<sup>[20]</sup> tuning important properties in cell development.

Preparing homogeneous biomolecular chimeras constitutes a major synthetic challenge.<sup>[21]</sup> Commonly, each biomolecule is prepared and functionalized with a handle followed by late-stage chemoselective conjugation. Alkyne-azide cycloaddition<sup>16,17</sup> is a prominent technique for protein- and peptide-glycan conjugation, among the numerous methods for selective protein modification (Scheme 1A).<sup>[24,25]</sup> The mild conditions required to preserve chemical integrity in the presence of multiple functional groups are chief obstacles.<sup>[24]</sup>

We aimed at creating lipid-peptide-glycan chimeras (LPGCs) by merging their syntheses to circumvent complications associated with late-stage conjugation. We envisioned that adjustments in automated glycan assembly (AGA) would allow for the execution of peptide couplings and generate LPGCs in a straightforward manner. The on-resin approach allowed oligosaccharide to be combined with other biomolecules for their presentation on nanostructured systems.

## Results and Discussion

### Design of Solid-phase Peptide-Glycan Chimera (PGC) Synthesis

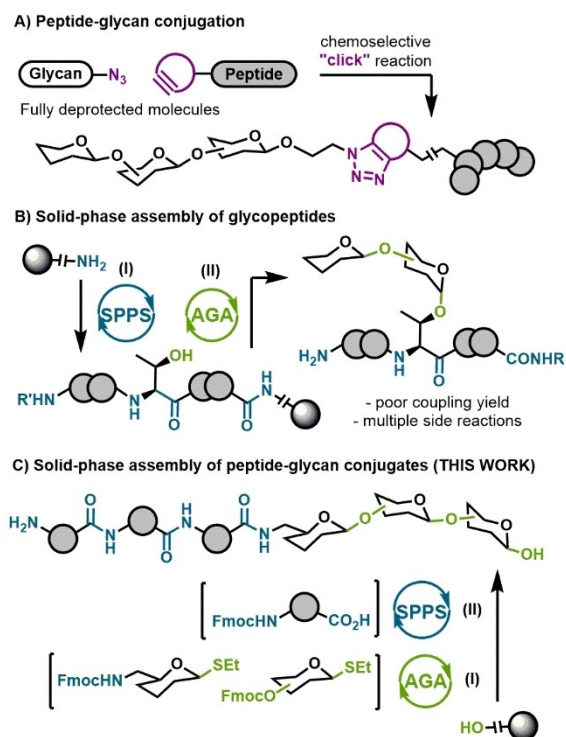
Glycopeptides are synthesized by incorporating glycosylated amino acid residues in the course of solid-phase peptide synthesis (SPPS).<sup>[26,27]</sup> In addition to inherent limitations associated with the complex and lengthy synthesis of these building blocks (BBs), poor conversion, racemization, and  $\beta$ -elimination render this method very case-dependent.<sup>[27]</sup> Currently, glycan assembly on resin-bound peptides is state-of-the-art (Scheme 1B). Few examples have been reported due to the need to subject the peptide to harsh glycosylation conditions.<sup>[28–30]</sup> Glycoside activation generally requires strong acids that are

[a] Dr. M. G. Ricardo, Prof. Dr. P. H. Seeberger  
Department of Biomolecular Systems  
Max-Planck-Institute of Colloids and Interfaces  
Am Muehlenberg 1, 14476 Potsdam (Germany)  
E-mail: peter.seeberger@mpikg.mpg.de

[b] Prof. Dr. P. H. Seeberger  
Institute of Chemistry and Biochemistry  
Freie Universitaet Berlin  
Arnimallee 22, 14195 Berlin (Germany)

Supporting information for this article is available on the WWW under <https://doi.org/10.1002/chem.202301678>

© 2023 The Authors. Chemistry - A European Journal published by Wiley-VCH GmbH. This is an open access article under the terms of the Creative Commons Attribution Non-Commercial NoDerivs License, which permits use and distribution in any medium, provided the original work is properly cited, the use is non-commercial and no modifications or adaptations are made.



**Scheme 1.** Synthetic methods used to prepare peptide-glycan chimeras. A) Late-stage conjugation of peptides and glycans by “click” reaction. B) Solid-phase synthesis of glycopeptides by assembling glycans on peptides. C) Combination of sequential automated glycan assembly and solid-phase peptide synthesis to obtain peptide-glycan chimeras.

often incompatible with the acid labile protecting groups masking the side chains in classic peptide synthesis.<sup>[29]</sup>

Here, the glycan portion of PGCs is synthesized by AGA before the peptide is constructed via SPPS. Thereby, the chimeric biomolecule can be assembled in a fully automated manner while interference of glycosylation conditions with the peptide is avoided completely (Scheme 1C). Whereas the resulting chimeras are structurally unrelated to natural glycopeptides, this strategy allows for the construction of more complex and larger heteropolymers. We sought the development of an amino-containing sugar BB that, after its incorporation at the end of an AGA protocol, enables the subsequent peptide synthesis. Monosaccharides bearing an Fmoc-protected amino group, similar to standard amino acid BBs used in SPPS, can be readily obtained following straightforward synthetic transformations (Scheme 2A). Mannose 6-NHFmoc-BB 5 resembles the 6-OFmoc-BB 7 and is expected to be compatible with conventional AGA. The assembly of these two BBs in the creation of a model mannose tetrasaccharide was envisioned to further evaluate peptide elongation (Scheme 2B).

### Automated Glycan Assembly

AGA was performed on Merrifield resin equipped with photocleavable linker 6 at 0.015 mmol scale in a home-built synthesizer.<sup>[31]</sup> Fmoc carbonate as a temporary protecting group

in BB 7 allowed for iterative glycan elongation. Benzyl (Bn) ethers and benzoyl (Bz) esters served as permanent protecting groups. Bz-protection of the C2-OH ensured selective trans-glycosylation. Glycan assembly relied on sequential cycles of acidic wash, glycosylation, capping, and Fmoc cleavage.

Incorporation of three units of 7 followed by one unit of BB 5 by AGA, afforded resin-bound glycan 8, as indicated by RP-HPLC and MALDI-MS analysis after microcleavage (Supporting Information). With the Fmoc-protected primary amine in place, peptide elongation was expected to proceed seamlessly, since the mild conditions required for amide bond formation would not impact the glycan structure.

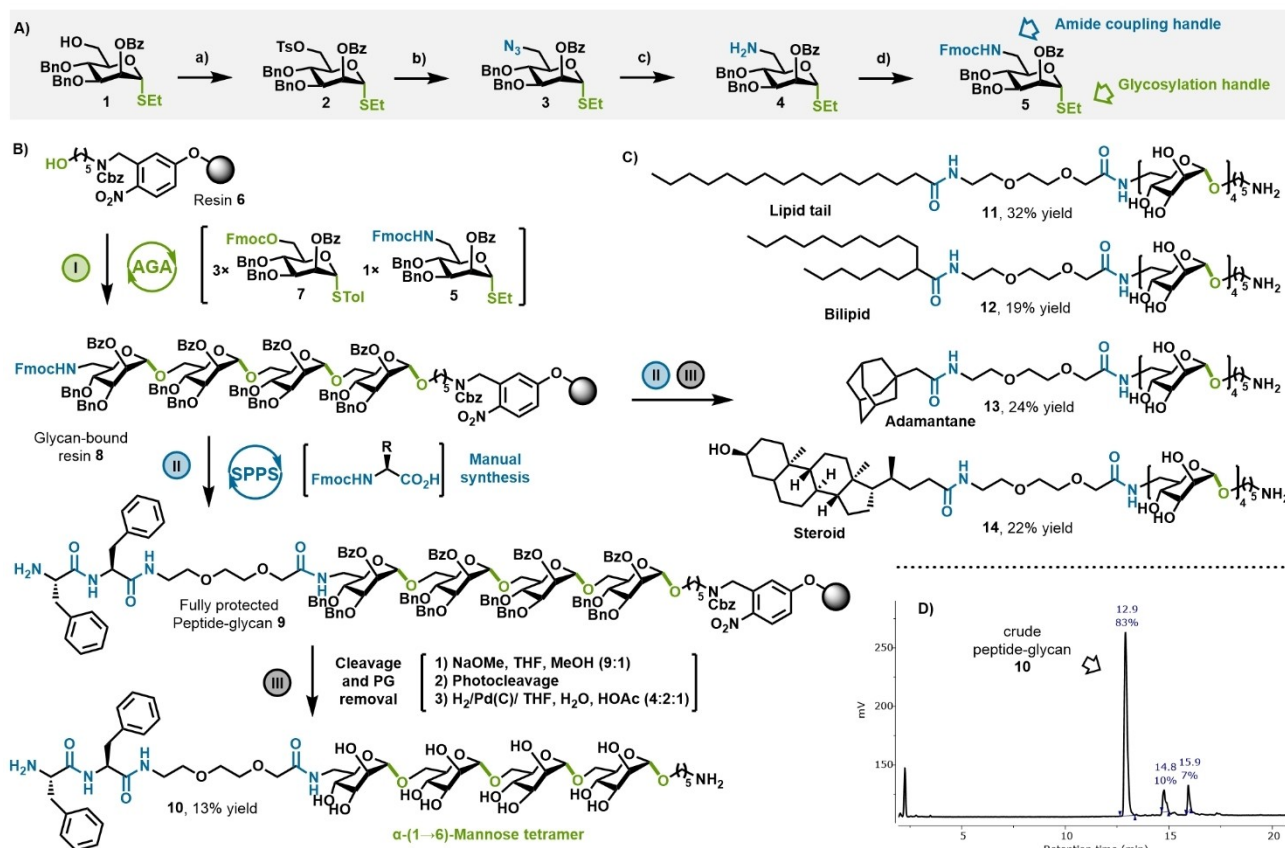
### Solid-Phase Peptide Synthesis

Following the completion of AGA, resin-bound glycan 8 is removed from the synthesizer and subjected to peptide synthesis. When only a few coupling reactions were needed, peptide synthesis on a manual setup was implemented using PyBOP/NMM activation. For longer peptides, the resin was transferred to an automated peptide synthesizer using a DIC/Oxyma activation strategy. Fmoc removal was achieved with piperidine (20% in DMF) in both setups.

Initially, we explored the incorporation of the dipeptide Phe-Phe (FF), that is frequently employed in supramolecular chemistry.<sup>[32]</sup> All glycans were equipped with a PEG-amino acid spacer prior to peptide assembly, to avoid interference between the biomolecules (Scheme 2B).<sup>[12]</sup> The successive coupling of two Phe units enabled the formation of fully protected resin-bound PGC 9, as indicated by MALDI-MS analysis (Supporting Information), showing no effect of peptide chemistry on the assembled glycan.

### Off-resin modifications

Benzoyl ester protecting groups were removed with sodium methoxide solution on resin. For optimal outcomes in the next steps, a careful selection of the solvent was required due to solubility issues. It was concluded that some acid in the reaction mixture was beneficial to avoid aggregate formation in chimeras prone to self-assembly. For photocleavage, an acidic solvent mixture (DCM: HFIP: TFA 100:10:1 (v/v/v)), ensured optimal results. The partially protected intermediates were subjected to hydrogenolysis to remove benzyl ethers and benzyl carbamate protecting groups under a hydrogen atmosphere using Pd(C) as a catalyst and an acidic solvent mixture of THF/H<sub>2</sub>O/AcOH 4:2:1 (v/v/v). Following these three synthetic steps, 9 was transformed into 10, obtaining 13% overall yield after one single purification by RP-HPLC. Combining AGA and SPPS for the preparation of FF-PEG2- $\alpha$ (1→6)-tetramannoside 10 yielded mainly the desired product according to HPLC analysis (Scheme 2D). The only two detectable by-products contained hydrogenated phenyl rings in the phenyl alanine side chains. This side reaction was completely avoided by reducing the hydrogenolysis time from 24 h to 6 h.



**Scheme 2.** Synthetic methods to generate lipid-peptide-glycan chimeras. A) Synthesis of a Fmoc-amino functionalized mannose building block 5: a) TsCl, 10% pyridine in DCM, overnight, 85%; b) NaN<sub>3</sub>, DMF, 80 °C, 6 h, 91%; c) Zn, THF: AcOH (10:1 v/v), overnight; d) FmocCl, pyridine, DCM, 6 h, 82% (two steps). B) Solid- and solution-phase methods for PGC synthesis. C) Extension of the AGA-SPPS approach to diversify glycans with steroid, lipid, and tag molecules. D) Analytic RP-HPLC of crude PGC 10 after all synthetic steps showing high conversion. PG = Protecting group.

### Synthesis of lipid-glycan chimeras

Lipidation strategies are used to facilitate the multivalent presentation of glycans in self-adjuncting vaccines.<sup>[33]</sup> Moieties other than amino acids possessing a carboxylic acid group can be incorporated into oligosaccharides with the new method, including a fatty acid (11) and a bilipid (12) (Scheme 2C). Adamantane-labeled glycan 13 has potential applications in supramolecular chemistry.<sup>[34]</sup> Glycan-steroid chimeras such as 14 were prepared by the assembly of lithocholic acid. Cleavage from the resin and protecting group removal generated the final chimeric molecules in more than 19% yield.

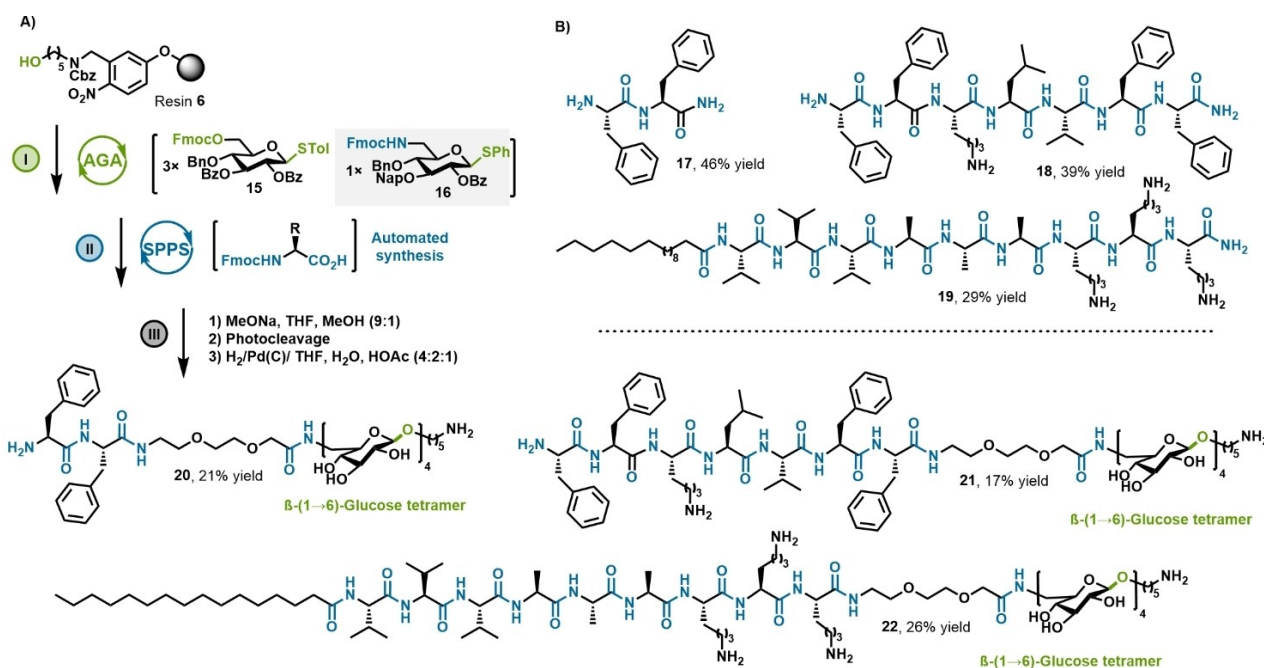
### Synthesis of self-assembling peptide-oligosaccharide chimeras

Synthetic peptides in combination with glycans open up opportunities for the creation of a multivalent environment with potential biomaterials applications. Nonetheless, access to such chimeras has been restricted to only a few examples of mono- and disaccharide-peptides chimeras due to the complex multistep syntheses required.<sup>[11–13,35]</sup> Our focus was directed to the design and synthesis of self-assembling peptide-oligosac-

charide chimeras. We sought to elucidate the morphology of such materials and the effect of glycan conjugation on the self-assembling features of peptides. In order to extend the present strategy to other oligosaccharides, an amino-containing glucose-BB 16 was prepared similar to mannose BB 5 (Supporting Information). This BB was inserted at the end of the AGA process to generate a model amino-containing  $\beta$ (1→6) tetraglucoside. The resin-bound glycan was used for SPPS of different fiber-forming peptides including FF, FFKLVFF, and palmitoyl-VVAAAKKK (Scheme 3A).

Dipeptide FF (17, Scheme 3B) was used in pioneering efforts to create nanostructured materials.<sup>[32,36]</sup> Its cationic form can result in a variety of structures from nanotubes to micelles depending on the concentration.<sup>[36]</sup> We investigated whether FF can transfer self-assembling features onto oligosaccharides. Similar to  $\alpha$ (1→6)tetramannoside 8 (Scheme 2B), after introducing the PEG2 spacer, two phenyl alanine residues were appended to  $\beta$ (1→6)tetraglucoside by manual peptide synthesis (Scheme 3A). Cleavage and protecting group removal, applying optimized conditions, afforded FF-PEG2- $\beta$ (1→6)tetraglucoside 20 in 21% yield without side reactions during hydrogenolysis.

The self-assembly properties of the A $\beta$  fragment (16–20) KLVFF and synthetic analogs have been studied in depth due to



**Scheme 3.** Chimeras of oligosaccharides and self-assembling peptides. A) Simplified methods for the synthesis of self-assembling peptide-tetraglycoside chimeras. B) Structures and overall yields of native self-assembling peptides synthesized by SPPS.

their role in amyloid fibrillation.<sup>[37,38]</sup> The extended derivative FFKLVFF<sup>[39]</sup> (**18**, Scheme 3B) benefits from its higher hydrophobicity and forms ribbon-like nanofibers in water when it is conjugated to PEG polymers.<sup>[40,41]</sup> In an attempt to reproduce this fiber-forming structure, by replacing the hydrophilic PEG chain with an oligosaccharide, FFKLVFF was assembled following AGA. Due to the higher number of amino acid residues, the peptide was elongated using an automated peptide synthesizer. Formation of the FFKLVFF-PEG2- $\beta$ (1 $\rightarrow$ 6) tetraglycoside **21** in 17% overall yield illustrates the compatibility of the automated protocols for glycan and peptide syntheses. The PGCs were synthesized and purified in less than 96 h.

Attaching a lipid tail to a  $\beta$ -sheet-forming peptide with a polar head of three Glu<sup>[42,43]</sup> or three Lys<sup>[19]</sup> residues results in a peptide amphiphile (PA) that self-assembles into nanofibers (Scheme 3B).<sup>[44,45]</sup> Merging a PA to peptide antigens such as RGD,<sup>[17,19]</sup> IKVAV,<sup>[17]</sup> and TSPHPV<sup>[43]</sup> has been explored more than glycans<sup>[12]</sup> or nucleic acid<sup>[20,46]</sup> antigens, as they can be prepared by automated peptide synthesis. With the present method, glycan and PAs can be assembled in a fully automated fashion as well. Thus, palmitoyl-VVVAACKK was appended onto  $\beta$ (1 $\rightarrow$ 6) tetraglycoside to finally yield 26% of lipid-peptide-glycan chimera **22** (Scheme 3A).

### Morphological studies

Self-assembly of peptides and the chimera was initially studied using atomic force microscopy (AFM) and circular dichroism (CD). For detailed analyses, selected samples were subjected to transmission electron microscopy (TEM). Samples from native

self-assembling peptides were prepared at 0.5 mM and 5 mM, then subjected to an annealing process by heating to 70 °C and slow cooling to room temperature. The aged samples were directly analyzed after 48 h.

The initial inspection of the structures formed by the native peptides (**17**, **18**, and **19**) suggested that the longer sequences were a better choice for the formation of the desired fibers. Dipeptide **17** did not show any supramolecular structure at 0.5 mM (Figure 1G) even after aging for up to five days, while spherical aggregates were observed at 5.0 mM in MeOH (Figure 1D). The longer FFKLVFF **18** at 5.0 mM in MeOH showed prominent fiber-like agglomerates (Supporting Information). Diluting the samples to 0.5 mM with water, was optimal for fiber formation, as shown by AFM (Figure 1E) and TEM measurements (Supporting Information). A similar behavior was observed for PA **19**, where a 0.5 mM solution in water showed a dense network of fibers as previously reported (Figure 1F).<sup>[19]</sup> The detailed characterization by TEM corroborates that **19** self-assembled into cylindrical fibers with high cohesion, while **18** formed a highly dispersed network of ribbon-twisted fibers (Supporting Information).

To compare the different propensities of peptides in inducing supramolecular assembly to the covalently attached glycan, all were subjected to identical protocols. Samples at 0.5 mM concentration were annealed and aged at room temperature for 48 h prior to the CD, AFM, and TEM analyses. Analogous to FF **17**, the FF-containing chimeras **10** and **20** showed no self-assembling behavior as indicated in AFM (Figure 1J, M). The CD analysis suggests that the presence of the oligosaccharide does not disturb the peptide conformation in solution (Figure 1A).



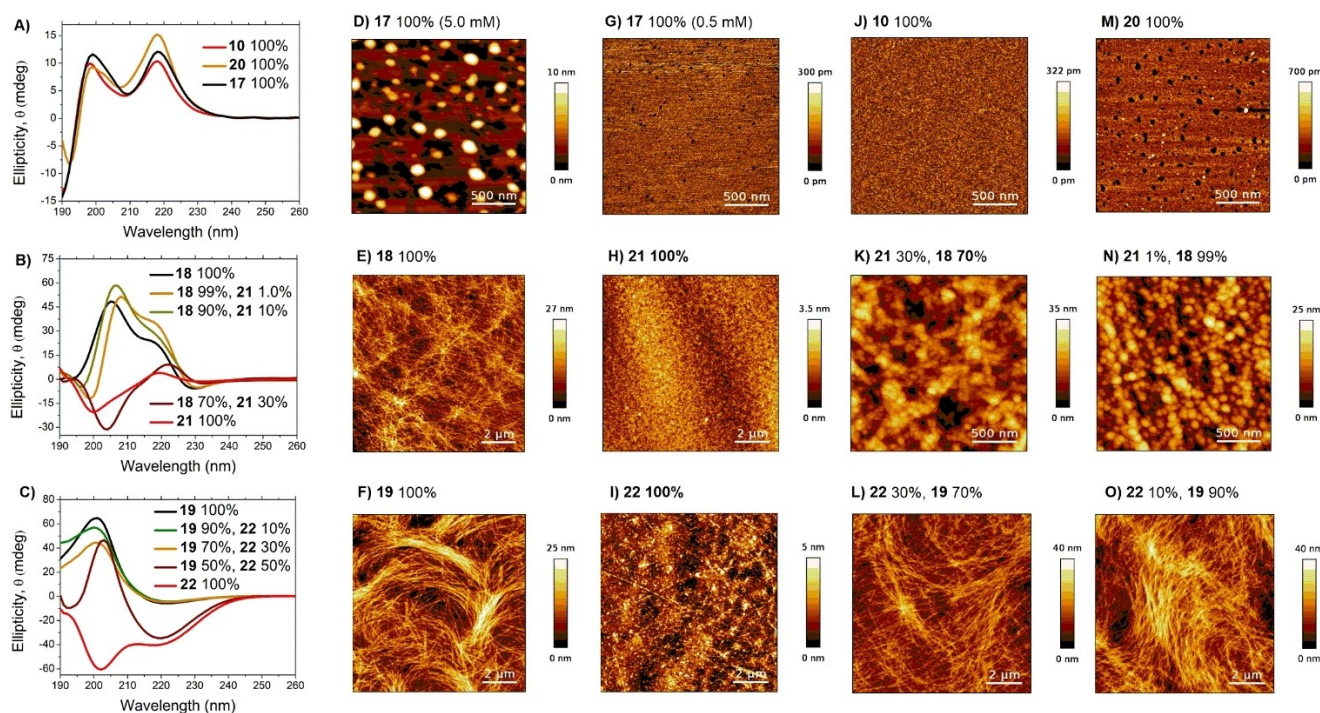


**Figure 1.** Structural and morphological analysis of pure PGCs and mixtures with the corresponding native peptides. A) to C) Circular dichroism comparison. D) to O) Images obtained by atomic force microscopy showing different morphologies. All samples analyzed correspond to 0.5 mM concentration, except for D) where 17 was analyzed at 5.0 mM.

In the case of pure FFKLVFF-based chimera 21, no self-assembling behavior was observed (Figure 1H), despite the clear fibers formed with pure peptide 18 (Figure 1E). These results were also validated by CD, where very different spectra were obtained, resembling a random coil peptide in pure 21 (Figure 1B). Aging the samples for more than one week did not promote the formation of aggregates. The large glycan may disturb peptide-peptide interactions that mediate fiber nucleation. Diluting 21 into the native self-assembling peptide 18 to diminish any glycan clashes, is a beneficial practice often applied to complex chimeras.<sup>[43,46]</sup> Mixing 21 and 18 (50%, 30%, 10%, and 1%) did not show any contribution to fiber formation (Supporting Information). Instead, at increasing dilution, the non-uniform aggregates observed at 50% and 30% ratios (Figure 1K) were gradually transformed into clear and homogeneous micelles at 1% (Figure 1N). PGC such as 21 may indeed aid in the desegregation of amyloid peptides, a phenomenon with implications in Alzheimer's disease.

Palmitoyl-VVAAAKK- $\beta$ (1–6)tetraglucoside 22 did not produce well-defined fibers but rather short fiber-like aggregates (Figure 1I). The presence of the glycans interferes with peptide-peptide assembly but does not block it like in the case of 21. Mixing 22 with 19 in different ratios resulted in the formation of fibers. The chimera/peptide ratio clearly affects fiber morphology. At a lower 22/19 ratio, fibers with high cohesion and the occasional presence of irregular clusters were generated similar to native 19 (Figure 1O). However, by increasing the content of 22, the fibers became longer and more defined, with an apparent optimum at around 30% (Figure 1L). The

steric demand of the attached glycan may disrupt peptide assembly at 50%. CD analysis shows similarities of the spectra at 10% and 30% ratios to pure 19 and a  $\beta$ -sheet pattern typical for these structures (Figure 1C). These glycan chimeras constitute novel synthetic materials with applications in biomaterial science.

## Conclusions

We present a general method for the straightforward chemical synthesis of lipid- and peptide-glycan chimeras combining solid-phase protocols. Merging solid-phase peptide synthesis with automated glycan assembly was accomplished by an amino-functionalized sugar monosaccharide. Thereby, glycans were readily derivatized by the introduction of an adamantane tag, lipids, and steroids. We developed the synthetic groundwork to merge oligosaccharides with self-assembling peptides. Inspired by the success of related biomaterials in nanotechnology, we were able to combine an oligosaccharide via a PEG spacer with peptides such as FF, FFKLVFF, and palmitoyl-VVAAAKK. Yields of around 20% after a single purification step and less than 96 h preparation time, highlight the robustness of the method. Initial examinations by AFM, and CD measurements, showed that neither the native FF peptide nor the two different chimeras resulted in supramolecular assembly. While the native FFKLVFF peptide forms a dense network of nanofibers, the assembly was completely suppressed when it was linked to an oligosaccharide. The effect of the glycan on

the peptide interaction was also observed when mixing the chimera with the native FFKLVFF peptide. Chimeras at a 1% ratio led to the supramolecular assembly of regular micelles, instead of fibers. The capability to merge biomolecules was demonstrated in the assembly of lipid-peptide-oligosaccharide chimeras that did not form uniform nanofibers on their own. Nevertheless, when they were present in a 30% ratio with respect to the native peptide, a clear and well-dispersed fiber network was obtained. These findings set the stage for the generation of biomaterials based on the conjugation of peptide amphiphiles with a host of different glycans.

## Experimental Section

All chemicals were reagent grade and used as supplied unless otherwise noted. All solvents for chemical reactions were commercially purchased in p.a. quality. BBs **6**, **7**, and **15** were acquired from GlycoUniverse GmbH & CO KGaA (Germany) while BBs **5** and **16** were synthesized as described in the Supporting Information. The construction of the lipid/peptide-glycan chimeras was performed on solid-phase, combining AGA followed by SPPS. AGA was performed using a home-built synthesizer developed at the Max Planck Institute of Colloids and Interfaces. Then, the glycan-bound resin is transferred to a peptide synthesizer (Liberty Blue, CEM) and the corresponding peptide or lipopeptide is assembled. When a small number of couplings were required (**10–14** and **20**), the peptide synthesis was performed manually. After cleavage and protecting group removal, the final PGC was purified by RP-HPLC and lyophilized. Final yields were calculated according to the initial resin loading. Detailed protocols of synthesis, characterization data, and morphological studies can be found in the Supporting Information.

**Automated glycan assembly:** AGA was performed at 0.015 mmol scale using resin **6** (43 mg, 0.35 mmol/g). The glycan elongation consisted of the iterative execution of the following protocols: *acidic wash* (1% TMSOTf/DCM), *thioglycoside glycosylation* (BB 0.1 mmol, NIS 0.1 mmol and TfOH 0.015 mmol in DCM/Dioxane 5:1 v/v), *capping* (MsOH: Ac<sub>2</sub>O: DCM 1:5:50, v/v/v) and *Fmoc removal* (20% piperidine in DMF).

**Manual solid-phase peptide synthesis:** Manual peptide synthesis was carried out at 0.015 mmol on glycan-bound resins (**10–14** and **20**). For peptide **17**, MBHA-S-RAM resin (Iris-Biotech, 0.50 mmol/g) was used at 0.2 mmol scale. Manual peptide couplings were performed by initially mixing the amino acid residue (8 equiv.), PyBOP (8 equiv.) and NMM (16 equiv.) in DMF. The mixture is pre-activated for 4 min, added to the resin, and the mixture is stirred at room temperature for 90 min. Fmoc removal was achieved with 20% piperidine in DMF (2×10 min).

**Automated solid-phase peptide synthesis:** Automated peptide elongation was implemented at 0.015 mmol scale for glycan-bound resins (**21** and **22**) and at 0.1 mmol scale on MBHA-S-RAM resin (0.50 mmol/g) for peptides (**18** and **19**). MW-assisted couplings in LibertyBlue synthesizer (CEM) were performed using the amino acid residue, DIC and Oxyma in five-fold excess, relative to the resin loading. Fmoc removal was achieved with 20% piperidine in DMF.

**Post-solid-phase methods:** Peptides **17**, **18**, and **19** were subjected directly to simultaneous cleavage and protecting group removal using TFA/TIS/H<sub>2</sub>O (95:2.5:2.5, v/v/v). For resins having lipid/peptide-glycan chimeras (**10–14** and **20–21**), it was required the execution of the following protocols: *On-resin methanolysis* (NaOMe in MeOH: THF 1:8 v/v, 0.06 M, overnight), *Photocleavage* (the resin

is suspended in TFA/HFIP/DCM 0.1:1:10 v/v/v and passed through a continuous flow photoreactor (0.3 mL/min, 360 nm, 450 W), and *Hydrogenolysis* (the crude is dissolved in THF: AcOH: H<sub>2</sub>O 4:1:2 v/v/v, Pd-C (10%, 0.2 g) is added and the reaction is stirred under H<sub>2</sub> atmosphere for 6 h).

**Peptide-glycan 10:** The combination of AGA (BBs 3×7 and 1×5) with manual SPPS afforded 2.3 mg (yield 13%). HR-MS m/z = 595.7766 [M + 2H]<sup>2+</sup>, calcd for C<sub>53</sub>H<sub>85</sub>N<sub>5</sub>O<sub>25</sub>: 595.7767.

**Lipid-glycan 11:** The combination of AGA (BBs 3×7 and 1×5) and manual SPPS afforded 5.5 mg (yield 32%). HR-MS m/z = 1134.6683 [M + H]<sup>+</sup>, calcd for C<sub>51</sub>H<sub>96</sub>N<sub>3</sub>O<sub>24</sub>: 1134.6384.

**Lipid-glycan 12:** The combination of AGA (BBs 3×7 and 1×5) with manual SPPS afforded 3.2 mg (yield 19%) HR-MS m/z = 1134.6591 [M + H]<sup>+</sup>, calcd for C<sub>51</sub>H<sub>96</sub>N<sub>3</sub>O<sub>24</sub>: 1134.6384.

**Adamantane-glycan 13:** The combination of AGA (BBs 3×7 and 1×5) with manual SPPS afforded 3.9 mg, yield 24%. HR-MS m/z = 1072.5499 [M + H]<sup>+</sup>, calcd for C<sub>47</sub>H<sub>82</sub>N<sub>3</sub>O<sub>24</sub>: 1072.5288.

**Steroid-glycan 14:** The combination of AGA (BBs 3×7 and 1×5) with manual SPPS afforded 4.1 mg (yield 22%). HR-MS m/z = 1254.7224 [M + H]<sup>+</sup>, calcd for C<sub>59</sub>H<sub>104</sub>N<sub>3</sub>O<sub>25</sub>: 1254.6959.

**Peptide 17:** Manual SPPS afforded 32 mg (yield 46%). HR-MS m/z = 334.1540 [M + Na]<sup>+</sup>, calcd for C<sub>18</sub>H<sub>21</sub>N<sub>3</sub>O<sub>2</sub>Na: 334.1531.

**Peptide 18:** Automated SPPS afforded 38 mg (yield 37%). HR-MS m/z = 473.7664 [M + 2H]<sup>2+</sup>, calcd for C<sub>53</sub>H<sub>73</sub>N<sub>9</sub>O<sub>7</sub>: 473.7816.

**Peptide 19:** Automated SPPS afforded 34 mg (yield 29%). HR-MS m/z = 384.2944 [M + 3H]<sup>3+</sup>, calcd for C<sub>58</sub>H<sub>114</sub>N<sub>13</sub>O<sub>10</sub>: 383.2859.

**Peptide-glycan 20:** The combination of AGA (BBs 3×15 and 1×16) with manual SPPS afforded 3.8 mg (yield 21%). HR-MS m/z = 595.7770 [M + 2H]<sup>2+</sup>, calcd for C<sub>53</sub>H<sub>85</sub>N<sub>5</sub>O<sub>25</sub>: 595.7767.

**Peptide-glycan 21:** The combination of AGA (BBs 3×15 and 1×16) with automated SPPS afforded 4.7 mg (yield 17%). HR-MS m/z = 609.3168 [M + 3H]<sup>3+</sup>, calcd for C<sub>88</sub>H<sub>134</sub>N<sub>11</sub>O<sub>30</sub>: 609.3099.

**Peptide-glycan 22:** The combination of AGA (BBs 3×15 and 1×16) with automated SPPS afforded 7.3 mg (yield 26%). HR-MS m/z = 507.9827 [M + 4H]<sup>4+</sup>, calcd for C<sub>93</sub>H<sub>177</sub>N<sub>15</sub>O<sub>33</sub>: 508.0658.

## Supporting Information

Additional references cited within the Supporting Information.<sup>[47–50]</sup>

## Abbreviations

AFM	Atomic Force Microscopy;
AGA	Automated Glycan Assembly
BB	Building Block
CD	Circular Dichroism
LPGC	Lipid Peptide Glycan Chimera
PA	Peptide Amphiphile
PEG	polyethylene glycol
SPPS	Solid-Phase Peptide Synthesis
TEM	Transmission Electron Microscopy

## Acknowledgements

We thank the Max-Planck Society for its generous financial support. Open Access funding enabled and organized by Projekt DEAL. Open Access funding enabled and organized by Projekt DEAL.

## Conflict of Interests

The authors declare no conflict of interest.

## Data Availability Statement

The data that support the findings of this study are available from the corresponding author upon reasonable request.

**Keywords:** biomaterials · glycan lipidation · peptide amphiphiles · peptide-glycan chimera · self-assembling

- [1] B. Leader, Q. J. Baca, D. E. Golan, *Nat. Rev. Drug Discovery* **2008**, *7*, 21–39.
- [2] A. Varki, *Glycobiology* **2017**, *27*, 3–49.
- [3] F. Berti, R. Adamo, *Chem. Soc. Rev.* **2018**, *47*, 9015–9025.
- [4] R. Roy, *Drug Discovery Today Technol.* **2004**, *1*, 327–336.
- [5] S. Achilli, N. Berthet, O. Renaudet, *RSC Chem. Biol.* **2021**, *2*, 713–724.
- [6] K. Zhou, H. Hong, H. Lin, L. Gong, D. Li, J. Shi, Z. Zhou, F. Xu, Z. Wu, J. Med. Chem. **2022**, *65*, 323–332.
- [7] P. J. McEnaney, C. G. Parker, A. X. Zhang, D. A. Spiegel, *ACS Chem. Biol.* **2012**, *7*, 1139–1151.
- [8] B. Liet, E. Laigre, D. Goyard, B. Todaro, C. Tiertant, D. Boturyn, N. Berthet, O. Renaudet, *Chemistry* **2019**, *25*, 15508–15515.
- [9] Y. Kim, J. Y. Hyun, I. Shin, *Chem. Soc. Rev.* **2021**, *50*, 10567–10593.
- [10] S. J. Richards, M. I. Gibson, *J. Am. Chem. Soc.* **2021**, *1*, 2089–2099.
- [11] E. Zacco, C. Anish, C. E. Martin, H. V. Berlepsch, E. Brandenburg, P. H. Seeberger, B. Koks, *Biomacromolecules* **2015**, *16*, 2188–2197.
- [12] S. S. Lee, T. Fyrner, F. Chen, Z. Álvarez, E. Sleep, D. S. Chun, J. A. Weiner, R. W. Cook, R. D. Freshman, M. S. Schallmo, K. M. Katchko, A. D. Schneider, J. T. Smith, C. Yun, G. Singh, S. Z. Hashmi, M. T. McClendon, Z. Yu, S. R. Stock, W. K. Hsu, E. L. Hsu, S. I. Stupp, *Nat. Nanotechnol.* **2017**, *12*, 821–829.
- [13] A. Restuccia, D. T. Seroski, K. L. Kelley, C. S. O'Bryan, J. J. Kurian, K. R. Knox, S. A. Farhadi, T. E. Angelini, G. A. Hudalla, *Commun. Chem.* **2019**, *2*, 53.
- [14] S. I. S. Hendrikse, L. Su, T. P. Hogervorst, R. P. M. Lafleur, X. Lou, G. A. Van Der Marel, J. D. C. Codee, E. W. Meijer, *J. Am. Chem. Soc.* **2019**, *141*, 13877–13886.
- [15] M. K. Müller, L. Brunsveld, *Angew. Chem. Int. Ed.* **2009**, *48*, 2921–2924.
- [16] S. Kiyonaka, K. Sada, I. Yoshimura, S. Shinkai, N. Kato, I. Hamachi, *Nat. Mater.* **2004**, *3*, 58–64.
- [17] G. A. Silva, C. Czeisler, K. L. Niece, E. Beniash, D. A. Harrington, J. A. Kessler, S. I. Stupp, *Science* **2004**, *303*, 1352–1355.
- [18] A. Dehsorkhi, V. Castelletto, I. W. Hamley, *J. Pept. Sci.* **2014**, *20*, 453–467.
- [19] F. Tantakitti, J. Boekhoven, X. Wang, R. V. Kazantsev, T. Yu, J. Li, E. Zhuang, R. Zandi, J. H. Ortony, C. J. Newcomb, L. C. Palmer, G. S. Shekhawat, M. O. De La Cruz, G. C. Schatz, S. I. Stupp, *Nat. Mater.* **2016**, *15*, 469–476.
- [20] C. M. Serrano, R. Freeman, J. Godbe, J. A. Lewis, S. I. Stupp, *ACS Appl. Bio Mater.* **2019**, *2*, 2955–2963.
- [21] B. Sarkar, N. Jayaraman, *Front. Chem.* **2020**, *8*, 1–27.
- [22] D. Goyard, A. M. S. Ortiz, D. Boturyn, O. Renaudet, *Chem. Soc. Rev.* **2022**, *51*, 8756–8783.
- [23] V. K. Tiwari, B. B. Mishra, K. B. Mishra, N. Mishra, A. S. Singh, X. Chen, *Chem. Rev.* **2016**, *116*, 3086–3240.
- [24] E. A. Hoyt, P. M. S. D. Cal, B. L. Oliveira, G. J. L. Bernardes, *Nat. Chem. Rev.* **2019**, *3*, 147–171.
- [25] O. Boutourea, G. J. L. Bernardes, *Chem. Rev.* **2015**, *115*, 2174–2195.
- [26] G. Arsequell, G. Valencia, *Tetrahedron: Asymmetry* **1997**, *8*, 2839–2876.
- [27] W. Doelman, S. I. Van Kasteren, *Org. Biomol. Chem.* **2022**, *20*, 6487–6507.
- [28] M. Hurevich, P. H. Seeberger, *Chem. Commun.* **2014**, *50*, 1851–1853.
- [29] H. Paulsen, A. Schleyer, N. Mathieux, M. Meldal, K. Bock, *J. Chem. Soc. Perkin Trans. 1* **1997**, 281–293. <
- [30] A. Schleyer, M. Meldal, R. Manat, H. Paulsen, K. Bock, *Angew. Chem. Int. Ed.* **1997**, *36*, 1976–1978.
- [31] L. Kröck, D. Esposito, B. Castagner, C. C. Wang, P. Bindschädler, P. H. Seeberger, *Chem. Sci.* **2012**, *3*, 1617–1622.
- [32] A. Levin, T. A. Hakala, L. Schnaider, G. J. L. Bernardes, E. Gazit, T. P. J. Knowles, *Nat. Chem. Rev.* **2020**, *4*, 615–634.
- [33] Y. Manabe, T. C. Chang, K. Fukase, *Drug Discovery Today Technol.* **2020**, *37*, 61–71.
- [34] A. Štimac, M. Šekutor, K. Mlinaric-Majerski, L. Frkanec, R. Frkanec, *Molecules* **2017**, *22*.
- [35] S. Ustun Yaylaci, M. Sardan Ekiz, E. Arslan, N. Can, E. Kilic, H. Ozkan, I. Orujalipoor, S. Ide, A. B. Tekinay, M. O. Guler, *Biomacromolecules* **2016**, *17*, 679–689.
- [36] X. Yan, Q. He, K. Wang, L. Duan, Y. Cui, J. Li, *Angew. Chem.* **2007**, *119*, 2483–2486.
- [37] M. J. Krysmann, V. Castelletto, A. Kelarakis, I. W. Hamley, R. A. Hule, D. J. Pochan, *Biochemistry* **2008**, *47*, 4597–4605.
- [38] J. Adamcik, V. Castelletto, S. Bolisetty, I. W. Hamley, R. Mezzenga, *Angew. Chem. Int. Ed.* **2011**, *50*, 5495–5498.
- [39] M. J. Krysmann, V. Castelletto, I. W. Hamley, *Soft Matter* **2007**, *3*, 1401–1406.
- [40] M. J. Krysmann, S. S. Funari, E. Canetta, I. W. Hamley, *Macromol. Chem. Phys.* **2008**, *209*, 883–889.
- [41] V. Castelletto, G. Cheng, S. Fuzeland, D. Atkins, I. W. Hamley, *Soft Matter* **2012**, *8*, 5434–5438.
- [42] E. T. Pashuck, H. Cui, S. I. Stupp, *J. Am. Chem. Soc.* **2010**, *132*, 6041–6046.
- [43] S. S. Lee, E. L. Hsu, M. Mendoza, J. Ghodasra, M. S. Nickoli, A. Ashtekar, M. Polavarapu, J. Babu, R. M. Riaz, J. D. Nicolas, D. Nelson, S. Z. Hashmi, S. R. Kaltz, J. S. Earhart, B. R. Merk, J. S. Mckee, S. F. Bairstow, R. N. Shah, W. K. Hsu, S. I. Stupp, *Adv. Healthcare Mater.* **2015**, *4*, 131–141.
- [44] M. P. Hendricks, K. Sato, L. C. Palmer, S. I. Stupp, *Acc. Chem. Res.* **2017**, *50*, 2440–2448.
- [45] J. R. Wester, J. A. Lewis, R. Freeman, H. Sai, L. C. Palmer, S. E. Henrich, S. I. Stupp, *J. Am. Chem. Soc.* **2020**, *142*, 12216–12225.
- [46] R. Freeman, M. Han, Z. Álvarez, J. A. Lewis, J. R. Wester, N. Stephanopoulos, M. T. McClendon, C. Lynsky, J. M. Godbe, H. Sangji, E. Luijten, S. I. Stupp, *Science* **2018**, *362*, 808–813.
- [47] A. Pardo-Vargas, M. Delbianco, P. H. Seeberger, *Curr. Opin. Chem. Biol.* **2018**, *46*, 48–55.
- [48] K. Daragics, P. Fügedi, *Tetrahedron* **2010**, *66*, 8036–8046.
- [49] W. A. Greenberg, E. S. Priestley, P. S. Sears, P. B. Alper, C. Rosenbohm, M. Hendrix, S. C. Hung, C. H. Wong, *J. Am. Chem. Soc.* **1999**, *121*, 6527–6541.
- [50] D. A. Williams, K. Pradhan, A. Paul, I. R. Olin, O. T. Tuck, K. D. Moulton, S. S. Kulkarni, D. H. Dube, *Chem. Sci.* **2020**, *11*, 1761–1774.

Manuscript received: June 10, 2023

Accepted manuscript online: June 26, 2023

Version of record online: August 25, 2023